

Asymmetries in Elastic Scattering of 100 MeV π^+ from a Polarized ^3He Target

B. Larson, O. Häusser, E. J. Brash, C. Chan, and A. Rahav
Simon Fraser University, Burnaby, British Columbia, Canada V5A 1S6

C. Bennhold, P. P. J. Delheij, R. S. Henderson, B. K. Jennings, A. Mellinger, D. Ottewell, A. Trudel,
 M. C. Vetterli, and D. M. Whittal^(a)
TRIUMF, 4004 Wesbrook Mall, Vancouver, British Columbia, Canada V6T 2A3

S. Ram
Tel-Aviv University, Ramat Aviv, Tel-Aviv 69 978, Israel

L. Tiator
Institut für Kernphysik, Universität Mainz, D6500 Mainz, Germany

S. S. Kamalov
Laboratory of Theoretical Physics, Joint Institute for Nuclear Research, Dubna, U.S.S.R.
 (Received 3 September 1991)

We report the observation of a large asymmetry in the elastic scattering of 100 MeV π^+ from a polarized ^3He target. Measurements have been made at laboratory angles of 60° , 80° , and 100° , with the largest value $A_y = 0.89 \pm 0.12$ occurring at 80° , near a cross-section minimum. This asymmetry is the largest observed to date in pion scattering from a spin- $\frac{1}{2}$ nucleus. The A_y data are qualitatively reproduced by a schematic model; however, agreement with the data is significantly improved when realistic three-body Faddeev wave functions and a full nonlocal distorted-wave impulse approximation reaction model are used.

PACS numbers: 25.80.Dj, 24.70.+s, 25.10.+s

Asymmetry measurements using polarized nuclear targets have only recently become feasible [1-3] and with the development of an optically pumped high-density polarized ^3He target [3] are possible even with pion fluxes of 10^6 - 10^7 s $^{-1}$. Measurements of this type provide valuable new information on the spin-dependent part of the π -nucleus scattering amplitude. Much theoretical work has gone into describing and understanding the π -nucleus interaction [4-8]. In general, predictions depend on the nuclear structure input, the elementary π -nucleon amplitudes, and the reaction model. For spin- $\frac{1}{2}$ targets in the $1p$ shell [1,2], ^{13}C and ^{15}N , relatively small asymmetries have been observed. A conclusive interpretation is made difficult by uncertainties in standard wave functions for the nuclear ground state, which give a poor description of the measured magnetic form factors, e.g., in ^{13}C [9] at momentum transfers $q \sim 2$ fm $^{-1}$. In contrast to this, the ^3He nuclear wave function can be calculated with good accuracy from the Faddeev equations using realistic NN potentials as input [10]. Therefore, for ^3He the nuclear structure uncertainties are almost negligible compared to p -shell nuclei and, furthermore, large asymmetries are expected. The $^3\text{He}(\pi^+, \pi^+)$ reaction is thus an ideal probe of the detailed spin dependence of the spin-0-spin- $\frac{1}{2}$ nuclear scattering amplitude [11-13].

The scattering amplitude for the $\pi^+ - ^3\text{He}$ system can be written as

$$t = f(\theta) + ig(\theta)\hat{n} \cdot \sigma, \quad (1)$$

where $f(\theta)$ is the non-spin-flip amplitude, $g(\theta)$ is the

spin-flip amplitude, and σ is the nuclear Pauli spin matrix. Defining \mathbf{k} and \mathbf{k}' as the momentum vectors of incoming and outgoing pions, respectively, the unit vector $\hat{n} \equiv \mathbf{k} \times \mathbf{k}' / |\mathbf{k} \times \mathbf{k}'|$ is in the direction perpendicular to the scattering plane. The differential cross section, $\sigma = |f|^2 + |g|^2$, is determined by the incoherent sum of the amplitudes, whereas the analyzing power, $A_y = 2 \text{Im}\{fg^*\}/\sigma$, is sensitive to the interference between them. In $\pi^+ - ^3\text{He}$ scattering the cross section depends strongly on the spin-dependent amplitude near the cross-section minimum [13] only, since g is near its maximum, f is near its minimum, and they are comparable in magnitude. The analyzing power has a strong dependence on the magnitude of g and on the relative phase between f and g even when the spin-flip amplitude is significantly smaller than the nonflip one.

The experiment was carried out at the M11 pion channel of the Tri-University Meson Facility (TRIUMF) using an optically pumped polarized ^3He target of 7.03 standard atm pressure and a typical polarization of 45%-55%. Momentum analysis of the scattered pions was performed with the quadrupole-quadrupole-dipole spectrometer [14]. Removal of both quadrupoles was necessary due to the spatial constraints imposed by the target and also for limiting magnetic-field gradients at the target to $< 3 \mu\text{Tcm}^{-1}$. This reduced the angular acceptance in the vertical (nonbend) plane to $\approx 3.5^\circ$, whereas the spectrometer angular acceptance in the horizontal (bend) plane was as large as 12° .

A detailed discussion of the TRIUMF polarized ^3He

target can be found elsewhere [3]. Briefly, the target consisted of an 8-cm-long \times 2.46-cm-inner-diam glass cell which contained 7.03 atm ^3He gas, a few mg of Rb alkali metal, and ≈ 100 Torr of N_2 quench gas. The glass cell was mounted in an oven made of the polyimide Vespel. Windows consisting of two layers of 25 μm Kapton separated by an air gap of $\frac{1}{4}$ in. were used to reduce heat loss and thermal gradients within the oven while contributing a minimal amount to the energy loss of the incident and scattered pions. The oven was operated at a temperature of 450 K to produce a Rb density of $\sim 4 \times 10^{14}$ cm^{-3} . About 7 W of circularly polarized photons ($\lambda = 795.8$ nm) were used to optically pump Rb via the D_1 line. A vertical holding field of 3 mT was produced by a set of 1-m-diam Helmholtz coils.

The target polarization produced by the Fermi-contact hyperfine interaction during Rb- ^3He spin-exchange collisions could be reversed and analyzed by adiabatic fast passage NMR. The NMR signal induced by the rotating ^3He magnetic moment was compared to that from a water sample of similar geometry to obtain an absolute value of the polarization. Because of the weakness of the water signal [it is smaller than the ^3He signal by a factor of $(3.71 \times 10^4)pP$, where p and P are the ^3He pressure and polarization, respectively] and a significant temperature dependence in the induced NMR signal, a systematic uncertainty of $\Delta P_i/P_i = 0.07$ has been adopted for the absolute ^3He polarization. This uncertainty is included in the overall systematic uncertainties for A_y quoted in Table I.

A total of four sets of multiwire proportional chambers (MWPC's), two placed in the pion beam directly in front of the target and two placed between the target and the spectrometer entrance, provided ray tracing to the target with 1–2 mm resolution. The tracking was essential to reject events which originated in the glass end caps and sidewalls of the target cell. Two different projections of the target image, a one-dimensional projection of the target cell onto the beam axis (z coordinate) and a two-dimensional projection of the cell onto the plane perpendicular to the beam axis (x - y plane), were used to identify the ^3He events. Software cuts on z eliminated events from the end caps while cuts on the cell-radius coordinate [$r = (x^2 + y^2)^{1/2}$] eliminated events from the cell walls. With the cuts from the tracking chambers the usable ^3He target length was 4.5 cm which corresponds to an areal

density of 8.5×10^{20} atoms cm^{-2} (4.26 mg cm^{-2}).

The two MWPC's located between the target and the spectrometer together with two additional chambers located after the spectrometer allowed us to determine the focal plane of the dipole. Events observed with a CH_2 target were used for momentum calibration of the focal plane and for normalizing the ^3He cross sections relative to the elementary π^+p reaction. A small scintillator placed directly upstream of the target cell defined the active area of the target, and in coincidence with a larger scintillator located downstream of the target was used to measure the total beam charge incident on the target cell. Normalized yield spectra for target spins up (σ_\uparrow) and down (σ_\downarrow) taken at $\theta_{\text{lab}} = 80^\circ$ are shown in the upper two frames of Fig. 1. The ^3He elastic peak has a width of about 3 MeV FWHM which arises from the energy spread of the incident beam (≈ 2 MeV) and from multiple scattering in the various detector and target elements. The target polarization labels (\uparrow and \downarrow) refer to a coordinate system in which the scattered pions are detected on the left side of the beam. The difference spectrum is shown in the bottom frame of Fig. 1. Since this difference is proportional to the analyzing power

$$A_y \approx \frac{1}{P_i} \frac{\sigma_\uparrow - \sigma_\downarrow}{\sigma_\uparrow + \sigma_\downarrow}, \quad (2)$$

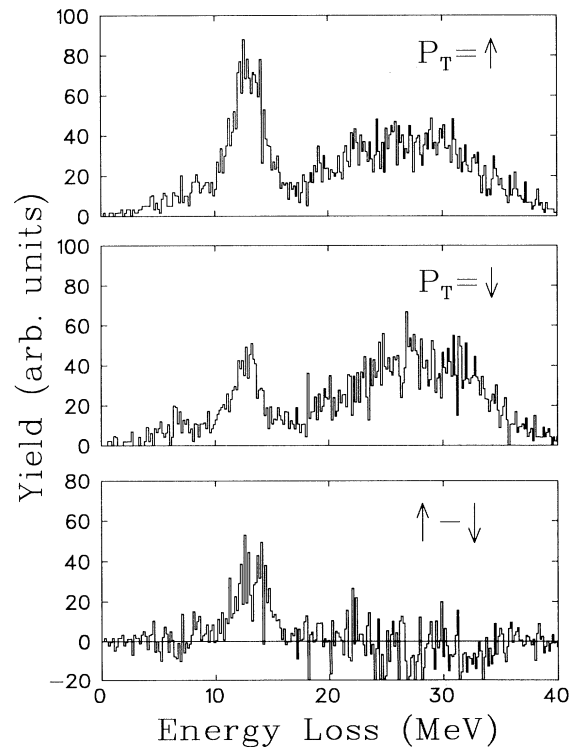


FIG. 1. Normalized yield spectra for the summed data at a laboratory angle of 80° . P_i indicates direction of the target polarization. The difference between the top two panels is shown in the bottom panel.

TABLE I. Cross sections and analyzing powers for 100 MeV $\pi^+ - ^3\text{He}$ elastic scattering.

$\theta_{\text{c.m.}}$ (deg)	$(d\sigma/d\Omega)_{\text{c.m.}}$ (mb/sr)	A_y
64.0	$1.8 \pm 0.08 \pm 0.36$	$0.04 \pm 0.09 \pm 0.02$
84.6	$0.7 \pm 0.04 \pm 0.14$	$0.89 \pm 0.12 \pm 0.10$
104.5	$2.1 \pm 0.06 \pm 0.42$	$0.38 \pm 0.06 \pm 0.04$

one can conclude that the background either is unpolarized or has an analyzing power close to zero. The systematic uncertainties quoted in Table I include the uncertainty from subtraction of this small background. To reduce systematic uncertainties due to long-term fluctuations of the target polarization, data were obtained in 3-h sets with polarization measurements between each set. The polarization was reversed every 12 h. Therefore several data sets were obtained for each angle and polarization state. This results in an overdetermined set of equations from which the asymmetry and cross section were extracted by a least-squares minimization of the function

$$\chi^2 = \sum_i \frac{[\sigma_i - \sigma_0(1 + A_y P_i)]^2}{(\Delta\sigma_i)^2}. \quad (3)$$

Here, σ and σ_0 are the measured polarized and unpolarized cross sections, respectively, P_i is the target polarization, A_y is the analyzing power, and the sum is over individual data sets i . The results are presented in Table I with the first error arising from counting statistics and the second from systematic uncertainties.

The measured experimental cross sections and asymmetries are compared to two different models. The full calculation employs realistic three-body wave functions for the initial and final states. This nuclear wave function has been obtained by solving the Faddeev equations with the Reid potential as the NN interaction [10]. Pion-nucleus scattering is then treated in the framework of multiple-scattering theory in which the π - ^3He scattering matrix $T(E)$ is given as a solution of the Lippmann-Schwinger equation [15]

$$T(E) = V(E) + V(E)G(E)T(E), \quad (4)$$

where $G(E)$ is the pion-nucleus Green's function. This equation is solved in momentum space and therefore treats nonlocalities exactly [13]. The potential matrix $V(E)$ is related to the free π - N t matrix and represents a first-order optical potential. A second-order term can, in principle, be added to $V(E)$ which represents true pion absorption and higher-order processes [15]. Such a phenomenological term was developed for heavier nuclei; however, its effects are shown to be small [16] for pion scattering and charge exchange on ^3He .

The full distorted-wave impulse approximation (DWIA) calculation is compared to a schematic model [17] in which the π^+ - ^3He non-spin-flip ($J=0$) and spin-flip ($J=1$) amplitudes are given by

$$\tilde{F} = (2f_{\pi^+p} + f_{\pi^+n})F_{J=0}(Q^2), \quad (5)$$

$$\tilde{G} = g_{\pi^+n}F_{J=1}(Q^2), \quad (6)$$

where $f_{\pi^+p,n}$ are the elementary π - N amplitudes [18] and the proton spins are assumed to be coupled to zero. At the momentum transfer range sampled here it is a good

approximation to assume

$$F_{J=0}(Q^2) = F_{J=1}(Q^2) = \exp(-r_0^2 Q^2/6)$$

with $r_0 = 1.65$ fm. Note that the elementary π - N amplitudes have been transformed from the π - N c.m. system to the π - ^3He c.m. system causing the angular distribution to be shifted about 10° lower in scattering angle.

Measured angular distributions of $d\sigma/d\Omega$ and A_y for π^+ - ^3He elastic scattering at 100 MeV are shown in Fig. 2 along with accurate cross-section data [19] of Källne *et al.* The error bars shown are the larger of either systematic or statistical errors. The data are compared to the full DWIA calculation (solid curve) and the schematic model (dashed curve). Both calculations produce similar results and, aside from an apparent angular shift, are in fair agreement with the data. The calculations predict the large A_y values observed experimentally; however, the schematic model fails to reproduce the cross section in the region of the minimum. In addition to the full DWIA and the schematic model, calculations were performed in the DWIA using only the S -state component of the trinucleon wave function [17]. The results were nearly the same as those of the full calculation. A large asymmetry

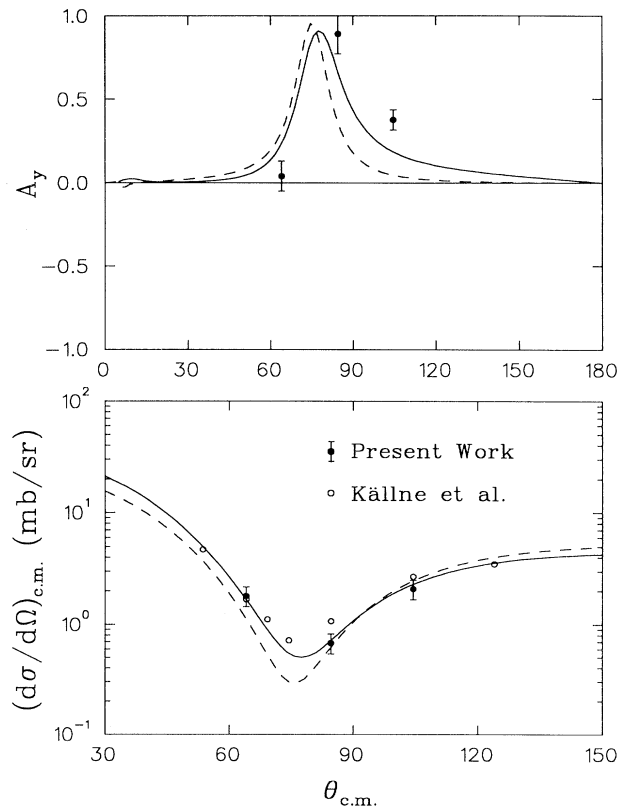


FIG. 2. A_y (top) and cross-section (bottom) angular distributions for elastic pion scattering on ^3He . The data are compared to a full DWIA calculation (solid curve) and a schematic model (dashed curve).

is also predicted by the momentum-space optical model of Landau [11], who used electromagnetic form factors to construct the required charge and spin densities in ${}^3\text{He}$.

Interpretation of the measurements is straightforward within the context of the simple model presented here [Eqs. (5) and (6)]. Since the nonflip elementary amplitudes are p wave dominated, they will go through zero at about 90° . The real and imaginary parts of f go through zero at different angles, however; therefore, $|f|$ is never equal to zero. Constructing the $\pi^+ - {}^3\text{He}$ amplitudes using Eqs. (5) and (6) one finds that $\text{Re}(\tilde{F})$ and $\text{Im}(\tilde{F})$ cross zero near 80° and 100° , respectively. One also finds that \tilde{F} and \tilde{G} are of comparable magnitude over this angular region. The only other requirement for a large asymmetry is that \tilde{F} and \tilde{G} be $\sim 90^\circ$ out of phase when they are of roughly equal magnitude since $A_y = 2 \times \text{Im}\{fg^*\}/\sigma$. The data indicate that these conditions are obviously met for the $\pi^+ - {}^3\text{He}$ system. Although the schematic model explains the existence of a large A_y near the cross-section minimum, the full calculation is clearly in better agreement with the data, especially at angles greater than 90° . This is a clear indication that details in the reaction model are important at this energy. The discrepancy between the two models can be traced to the imaginary part of g . It is this enhanced sensitivity of A_y to the spin-flip amplitude that makes asymmetry measurements valuable.

Calculations for $\pi^- - {}^3\text{He}$ scattering yield similar agreement between the two models; however, the analyzing powers are predicted to be only about half as large. An experiment to measure the asymmetry for π^- scattering at 100 MeV is planned at TRIUMF. It will also be of interest to study the energy dependence of the $\pi^- - {}^3\text{He}$ interaction. At energies above the Δ resonance the full calculation predicts large negative values of A_y , whereas in the schematic model this change of sign across the resonance is *not* predicted. This is an indication that multiple scattering and absorption effects are more important at the higher energies.

In summary, we have presented the first measurement of A_y in elastic pion scattering from polarized ${}^3\text{He}$. The results are in contrast to the rather small asymmetries observed in recent measurements with polarized targets of ${}^{13}\text{C}$ [6] and ${}^{15}\text{N}$ [7]. In the $\pi^- - {}^3\text{He}$ system several different models predict large asymmetries and, furthermore, show a distinct lack of sensitivity to nuclear struc-

ture details. Although the angular position of the peak in the asymmetry is not quite reproduced by the full DWIA calculation, inclusion of multiple scattering and absorption in the reaction model significantly improves the agreement with the experiment.

This work was supported by grants from the Natural Sciences and Engineering Research Council of Canada.

^(a)Permanent address: National Accelerator Centre, Faure, 7131, South Africa.

- [1] Yi-Fen Yen *et al.*, Phys. Rev. Lett. **66**, 1959 (1991).
- [2] R. Tacik *et al.*, Phys. Rev. Lett. **63**, 1784 (1989).
- [3] B. Larson *et al.*, Phys. Rev. A **44**, 3108 (1991).
- [4] R. H. Landau, S. C. Pathak, and F. Tabakin, Ann. Phys. (N.Y.) **78**, 299 (1973).
- [5] R. H. Landau and A. W. Thomas, Nucl. Phys. **A302**, 461 (1978).
- [6] M. Wakamatsu, Nucl. Phys. **A340**, 280 (1980).
- [7] D. J. Ernst, in *Proceedings of the LAMPF Workshop on Physics with Polarized Targets, Los Alamos, New Mexico, 1986* (LANL Report No. LA-10772-C, 1986), p. 129.
- [8] R. Mach and S. S. Kamalov, Nucl. Phys. **A511**, 601 (1990).
- [9] R. S. Hicks *et al.*, Phys. Rev. C **26**, 339 (1982).
- [10] R. A. Brandenburg, Y. E. Kim, and A. Tabis, Phys. Rev. C **12**, 1368 (1975).
- [11] R. H. Landau, Phys. Rev. C **15**, 2127 (1977).
- [12] F. M. M. Van Geffen *et al.*, Nucl. Phys. **A468**, 683 (1987).
- [13] S. S. Kamalov, L. Tiator, and C. Bennhold, Few-Body Syst. (to be published).
- [14] R. J. Sobie *et al.*, Nucl. Instrum. Methods **219**, 501 (1984).
- [15] M. Gmitro, S. S. Kamalov, and R. Mach, Phys. Rev. C **36**, 1105 (1987); M. Gmitro, J. Kvasil, and R. Mach, Phys. Rev. C **31**, 1349 (1985).
- [16] L. Tiator, C. Bennhold, and S. S. Kamalov, in *Proceedings of the International Workshop on Pions in Nuclei, Peniscola, Spain, 1991* (to be published).
- [17] C. Bennhold, B. K. Jennings, L. Tiator, and S. S. Kamalov (to be published).
- [18] R. A. Arndt and L. D. Soper, Scattering Analysis Interactive Dial-In (SAID) program, π - N scattering solutions.
- [19] J. Källne, J. F. Davis, J. S. McCarthy, R. C. Minehart, R. R. Whitney, R. L. Boudrie, J. B. McClelland, and A. Stetz, Phys. Lett. **103B**, 13 (1981).